JOURNAL OF SOLID STATE CHEMISTRY 99, 267–275 (1992)

Spin Glass Behavior in Sr_3FeRuO_7 and Sr_4FeRuO_8

P. D. BATTLE,* S. K. BOLLEN, AND A. V. POWELL

Inorganic Chemistry Laboratory, South Parks Road, Oxford, OX1 3QR, England

Received October 30, 1991; accepted January 28, 1992

The crystal structure of the new Ruddlesden–Popper phase Sr_3FeRuO_7 has been refined from neutron powder diffraction data collected at 1.7 K; space group *I4/mmm*, $a = 3.9187(1)$, $c = 20.4146(3)$ Å. The crystal structure of the K_2NiF_4-like compound Sr_4FeRuO_8 has also been refined; space group *I4/mmm*, $a = 3.9025(1)$, $c = 12.5943(3)$ Å. Neither compound appears to be magnetically ordered at 1.7 K. However, the magnetic susceptibilities of Sr_3FeRuO_7 and Sr_4FeRuO_8 have maxima at 23 K and 11 K, respectively, and show hysteresis effects below these temperatures. This behavior is interpreted in terms of magnetic frustration arising from the presence of competing superexchange interactions between Fe^{3+} and Ru^{5+} cations in nearest-neighbor and next-nearest-neighbor sites.

Introduction

In the course of a research program designed to investigate the electronic properties of cations from the second transition series, we have previously studied the magnetic behavior of Sr_2FeRuO_6 (*1*). This compound has a perovskite-like crystal structure, with a disordered distribution of $Fe^{3+}:3d^5$ and $Ru^{5+}:4d^3$ cations over the six-coordinate (B) sites. The magnetic susceptibility of our sample reached a maximum at ca. 50 K, and was history-dependent below this temperature. In particular, data measured on warming the sample from 4.2 K following cooling in zero applied magnetic field (zfc) did not overlay those collected after cooling in the measuring field (fc). Despite the maximum in the susceptibility, neutron powder diffraction data collected at a temperature of 5 K contained no Bragg scattering that was attributable to the presence of long-range magnetic order. A six-line ^{57}Fe Mössbauer spectrum was observed at 4.2 K, but the temperature dependence of the spectrum suggested that although at 4.2 K the spin system was static on the Mössbauer timescale, the hyperfine splitting was not associated with long-range magnetic order. These observations led us to describe Sr_2FeRuO_6 as a spin glass. The transition-metal sublattice in a perovskite is essentially simple cubic, although in Sr_2FeRuO_6 there is a small, monoclinic distortion. This is not a topologically frustrated system, nor is the six-coordinate sublattice magnetically dilute in our compound. In order to explain our observations we therefore considered the different magnetic superexchange interactions that can occur between nearest-neighbor Fe^{3+} and Ru^{5+} cations,

To whom correspondence should be addressed.

0022-4596/92 $5.00

randomly distributed over a simple cubic lattice. The coupling between pairs of Fe^{3+} ions, and between pairs of Ru^{5+} ions, is expected to be antiferromagnetic, but the coupling between the $3d^5$ and $4d^3$ ions along a 180° superexchange pathway will be ferromagnetic (*2*). Our model for the unusual behavior of Sr_2FeRuO_6 relied on the presence of both types of interaction, an idea that was supported by the observation of long-range magnetic order in related Ru^{5+} oxides which do not contain a second magnetic species. However, the model was not entirely satisfactory because, if only nearest-neighbor interactions are significant, the perovskite structure is not frustrated even when both ferromagnetic and antiferromagnetic coupling are present. The average ordered magnetic moment per cation site (the quantity measured in a neutron diffraction experiment) is then given by $(\mu_{Fe} - \mu_{Ru})/2$, where μ_{Fe} is the ordered magnetic moment of an Fe^{3+} ion and μ_{Ru} is the ordered moment of an Ru^{5+} ion. This quantity would be expected to have a value of ca. 1 μ_B in Sr_2FeRuO_6 and, although this is quite close to the sensitivity limit of our experiment, it is somewhat surprising that we were unable to detect any magnetic Bragg scattering. We now believe that we were right to make the coexistence of ferromagnetic and antiferromagnetic superexchange the cornerstone of our model, but that we must include interactions between more distant neighbors in order to explain our data fully. In this paper we describe neutron diffraction and magnetic susceptibility experiments on Sr_3FeRuO_7, a new compound having the Ruddlesden–Popper (RP) structure (*3*), and Sr_4FeRuO_8, reported previously (*4*) as a K_2NiF_4 structure. We hoped that a study of the magnetic properties of these two materials would lead to a better understanding of the interaction between Ru^{5+} and Fe^{3+}. Figure 1 shows the structural relationship between the three compounds; the perovskite is a three-dimensional solid, whereas the K_2NiF_4 structure is effectively a two-dimensional layer structure. The RP structure is intermediate between the two.

Experimental

Polycrystalline samples of the title compounds were prepared by firing pelletized stoichiometric quantities of $SrCO_3$, Fe_2O_3, and dried RuO_2 (all from Johnson Matthey Chemicals) in air at temperatures of 1200°C for Sr_4FeRuO_8 and 1400°C for Sr_3FeRuO_7. The progress of the reactions was monitored by X-ray powder diffraction, performed at room temperature using Ni-filtered Cu$K\alpha$ radiation. A single phase sample of Sr_4FeRuO_8 was obtained after a few days, whereas a firing time of several weeks was necessary in the case of Sr_3FeRuO_7. The reactions were carried out in alumina crucibles and the samples were cooled to room temperature simply by removing them from the furnace. The pellets were well sintered at the end of the reaction. Neutron powder diffraction data were collected on both compounds at a temperature of 1.7 K using the diffractometer D1a at ILL Grenoble. The angular range $6 < 2\theta < 144°$ was scanned with a step size of 0.05° using a neutron wavelength of 1.9116 Å (Sr_3FeRuO_7) or 1.9127 Å (Sr_4FeRuO_8). The samples were contained in vanadium cans which were mounted in an Al-tailed cryostat. Magnetic susceptibility measurements were made in the temperature range $7 < T < 300$ K using a Cryogenics SCU500 SQUID magnetometer. Data were recorded after cooling the samples in zero field (zfc) and after cooling in the measuring field of 0.5 T (fc). The thermal remanent magnetization (TRM) was measured for both samples and its temperature dependence was followed in the case of Sr_3FeRuO_7.

Results

Our X-ray powder diffraction studies showed that Sr_3FeRuO_7 has a body-cen-

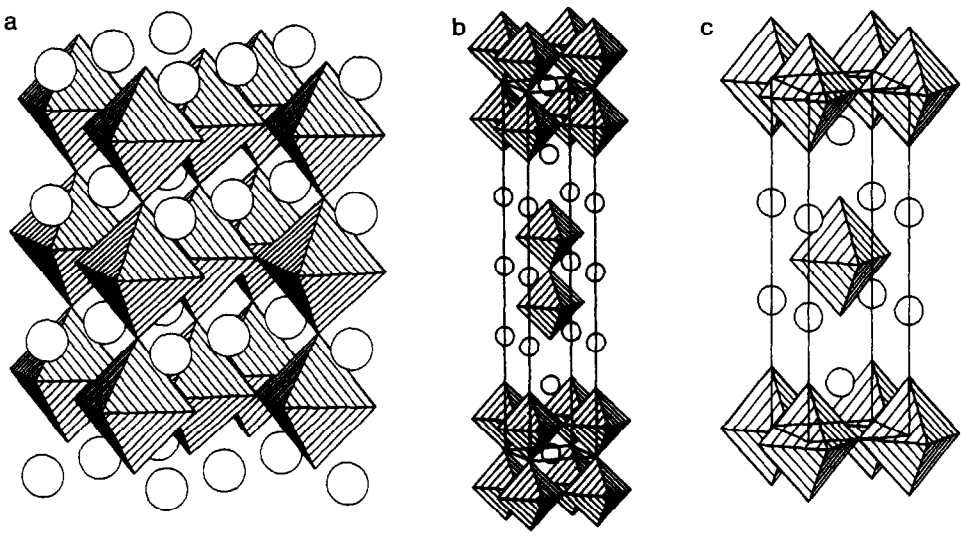

FIG. 1. (a) The perovskite structure of Sr_2FeRuO_6, (b) the Ruddlesden–Popper structure of Sr_3FeRuO_7, and (c) the K_2NiF_4 structure of Sr_4FeRuO_8. Fe/RuO_6 octahedra are shaded; Sr atoms are drawn as hollow circles.

tered tetragonal unit cell with $a = 3.921(1)$, $c = 20.411(5)$ Å, and thus suggested (*3*) that we had achieved our aim of preparing a Ruddlesden–Popper phase in the Sr–Fe–Ru–O system. The X-ray pattern of Sr_4FeRuO_8 showed the same symmetry, as would be expected for a K_2NiF_4 phase. The values of the unit-cell parameters ($a = 3.9135(8)$, $c = 12.616(3)$ Å) were slightly larger (0.2%) than those reported (*4*) when this compound was first prepared. The low-temperature neutron diffraction data were analyzed using the Brookhaven profile refinement program (*5, 6*) with the following scattering lengths: $b_{Sr} = 0.70$, $b_{Fe} = 0.95$, $b_{Ru} = 0.73$, and $b_O = 0.58 \times 10^{-12}$ cm. The background level was estimated by interpolation between regions where there were no Bragg peaks, and the latter were assumed to have a pseudo-Voigtian line profile. Both data sets were analysed using the tetragonal space group *I4/mmm*. There was no need to allow for the presence of magnetic Bragg scattering in order to account for the observed diffraction patterns. In view of the layered nature of the crystal structures, anisotropic temperature factors were used to describe the thermal motion of the atoms. Trial refinements suggested that there was not a significant concentration of anion vacancies in either compound, nor was there any evidence for long range ordering of the Fe and Ru cations over the six-coordinate sites. Our final data analysis thus assumed a disordered arrangement of the transition-metal ions. Refinement of 17 atomic parameters resulted in *R*-factors of $R_{wpr} = 4.48$, $R_I = 1.5\%$ in the case of Sr_3FeRuO_7. The final atomic coordinates are listed in Table I and the corresponding bond lengths and bond angles are presented in Table II. There are two crystallographically distinct strontium atoms in the asymmetric unit; Sr1 lies within the double perovskite layers, whereas Sr2 lies in the interlayer gap (Fig. 1). Similarly, O1 is located at the center of the double layers, O2 lies (approximately) in the same *xy* plane as the transition-metal ions, and O3 is situated on the outer edge of the double layers. The final observed and calculated

TABLE I

STRUCTURAL PARAMETERS FOR Sr_3FeRuO_7 AT 1.7 K (SPACE GROUP *I4/mmm*)

Atom	Site	x	y	z	B_{11} (Å^2)	B_{22} (Å^2)	B_{33} (Å^2)
Sr1	2*b*	0	0	½	0.13(3)	0.13(3)	0.20(8)
Sr2	4*e*	0	0	0.31581(5)	0.18(0)	0.18(0)	0.22(0)
Fe/Ru	4*e*	0	0	0.09869(4)	0.02(2)	0.02(2)	0.66(3)
O1	2*a*	0	0	0	0.85(4)	0.85(4)	0.42(10)
O2	8*g*	0	¼	0.09546(5)	0.19(3)	0.08(3)	0.68(4)
O3	4*e*	0	0	0.19537(5)	0.16(3)	0.16(3)	0.39(6)

Note. a = 3.9187(1), c = 20.4146(3) Å.

TABLE III

STRUCTURAL PARAMETERS FOR Sr_4FeRuO_8 AT 1.7 K (SPACE GROUP *I4/mmm*)

Atom	Site	x	y	z	B_{11} (Å^2)	B_{22} (Å^2)	B_{33} (Å^2)
Sr	4*e*	0	0	0.35517(9)	0.00(2)	0.00(2)	0.25(5)
Fe/Ru	2*a*	0	0	0	0.29(3)	0.29(3)	0.64(6)
O1	4*e*	0	0	0.15954(10)	0.28(3)	0.28(3)	0.49(7)
O2	4*c*	½	0	0	0.30(6)	0.36(5)	0.52(6)

Note. a = 3.9025(1), c = 12.5943(3) Å.

diffraction profiles are plotted in Fig. 2. *R*-factors of R_{wpr} = 4.67, R_I = 2.76% were obtained after the refinement of the 11 atomic parameters which define the structure of Sr_4FeRuO_8. Their final values are listed in Table III, and the most important bond lengths are given in Table IV. Here O1 is the apical oxygen atom and O2 the equatorial. The observed and calculated diffraction profiles are drawn in Fig. 3. The results of our magnetic susceptibility measurements on Sr_3FeRuO_7 are plotted in Fig. 4. The zfc and the fc data are in excellent agreement above 23 K, at which temperature there is clearly a magnetic phase transition. Taken alone, the zfc data suggest that the transition is from a paramagnetic phase to an antiferromagnetic phase. However, the divergence of the two curves suggests that the low-temperature phase is not a classical Néel antiferromagnet, but that a fraction of the spins are decoupled in some way. Furthermore, the nonlinearity of the reciprocal susceptibility with temperature shows that this material is not a true Curie–Weiss paramagnet in the high-temperature region. Analysis of the data at $T > 200$ K leads to an intercept on the horizontal axis of $\theta = -130$ K and a molar Curie constant of 3.37 emu. The latter can be compared to a theoretical, spin-only value of 6.25. The corresponding data for Sr_4FeRuO_8 are plotted in Fig. 5. The low-temperature divergence of the zfc and fc data is more marked in this case, with the transition temperature taking a somewhat lower value (11 K), as might be expected in view of the low dimensionality of the crystal structure. Again the inverse susceptibility is a nonlinear function of temperature, with the best extrapolation from high temperatures leading to the values $\theta = -155$ K and C = 3.89 emu. The observation of thermal remanent magnetization in Sr_3FeRuO_7 is further evidence of a complex magnetic behavior; the data (Fig. 6) indicate a transition tempera-

TABLE II

BOND LENGTHS (Å) AND BOND ANGLES (Deg) FOR Sr_3FeRuO_7 AT 1.7 K

		Bond lengths		
			Sr2–O2	2.669(1) × 4
Sr1–O1	2.771 × 4		Sr2–O3	2.459(1) × 1
Sr1–O2	2.763(1) × 8		Sr2–O3	2.780(1) × 4
Mean Sr1–O	2.766		Mean Sr2–O	2.695
Fe/Ru–O1	2.015(1)			
Fe/Ru–O2	1.960(1) × 4		Mean Fe–O	1.972
Fe/Ru–O3	1.974(1)			
		Bond angles		
O2–Fe/Ru–O1	88.1		O3–Fe/Ru–O2	91.9
O2–Fe/Ru–O2	89.9		Fe/Ru–O2–Fe/Ru	176.1

TABLE IV

BOND LENGTHS (Å) FOR Sr_4FeRuO_8 AT 1.7 K

Sr–O1	2.464(2)	Sr–O2	2.671(1) × 4
Sr–O1	2.766(2) × 4		
Mean Sr–O	2.690		
Fe/Ru–O1	2.009(1) × 2	Fe/Ru–O2	1.951 × 4
mean Fe–O	1.970		

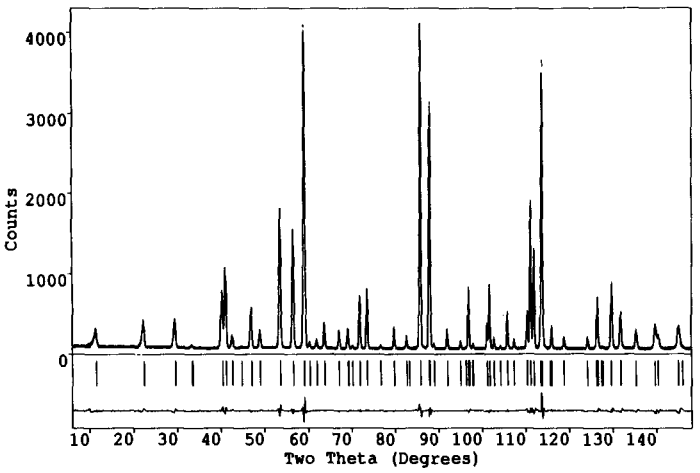

FIG. 2. The observed (....), calculated (__), and difference neutron powder diffraction profiles of Sr_3FeRuO_7 at 1.7 K. Reflection positions are marked.

ture that agrees well with that derived from the results of the susceptibility measurements. The TRM of Sr_4FeRuO_8 was 286 Am^{-1} at 7 K and decreased rapidly to zero with increasing temperature.

Discussion

The formation of a Ruddlesden–Popper phase in the Sr–Fe–Ru–O system was anticipated in view of the existence of both the perovskite Sr_2FeRuO_6 and the layer structure Sr_4FeRuO_8. However, a high temperature and a long reaction time were necessary in order to prepare a monophasic sample of the RP intermediate composition. The average coordination geometry about the transition-metal site is somewhat irregular, as is usual in RP phases (*7*), but the mean Fe/Ru–O distance is the same as that found

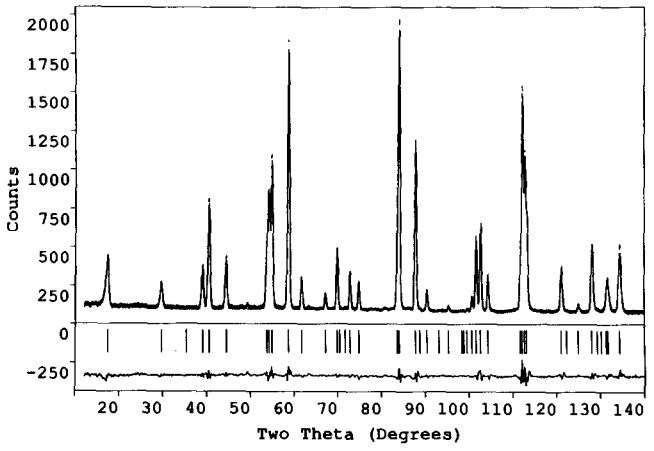

FIG. 3. The observed (....), calculated (__), and difference neutron powder diffraction profiles of Sr_4FeRuO_8 at 1.7 K. Reflection positions are marked.

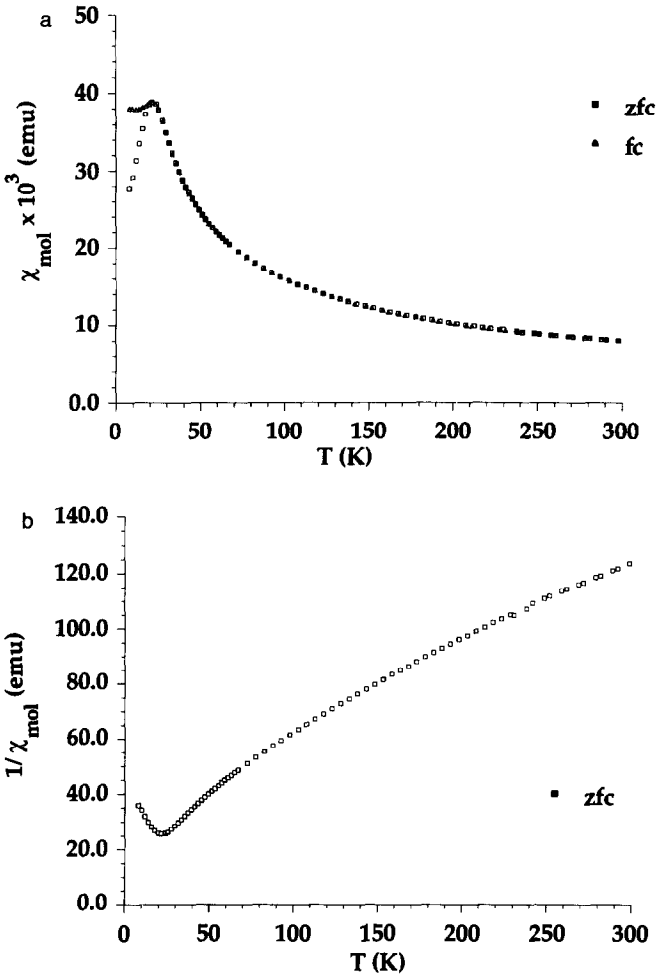

FIG. 4. (a) The zfc and fc molar magnetic susceptibility of Sr_3FeRuO_7 and (b) the zfc reciprocal susceptibility as a function of temperature.

(*1*) in Sr_2FeRuO_6. Similarly, the Fe/Ru–O_6 octahedra in Sr_4FeRuO_8 show a marked tetragonal distortion but the average metal-to-oxygen distance is again 1.97 Å. Clearly we are dealing with three compounds in which the overall crystal structure shows a varying dimensionality, but with a local cation environment that is essentially constant. The high symmetry of these structures leads to near-linear Fe/Ru–O2–Fe/Ru magnetic superexchange pathways between nearest-neighbor cations and hence a careful consideration of the magnetic properties is possible. The most interesting aspect of the results described above is indeed the apparent lack of long-range magnetic order in Sr_3FeRuO_7 and Sr_4FeRuO_8, as shown by the neutron diffraction data, despite the observation of a low-temperature maximum in the zfc magnetic susceptibility and, in the case of Sr_4FeRuO_8 (*4*), the presence of a hyperfine field in the Mössbauer spectrum at 4.2 K. The low Curie constants and the high, negative θ values derived in both cases from

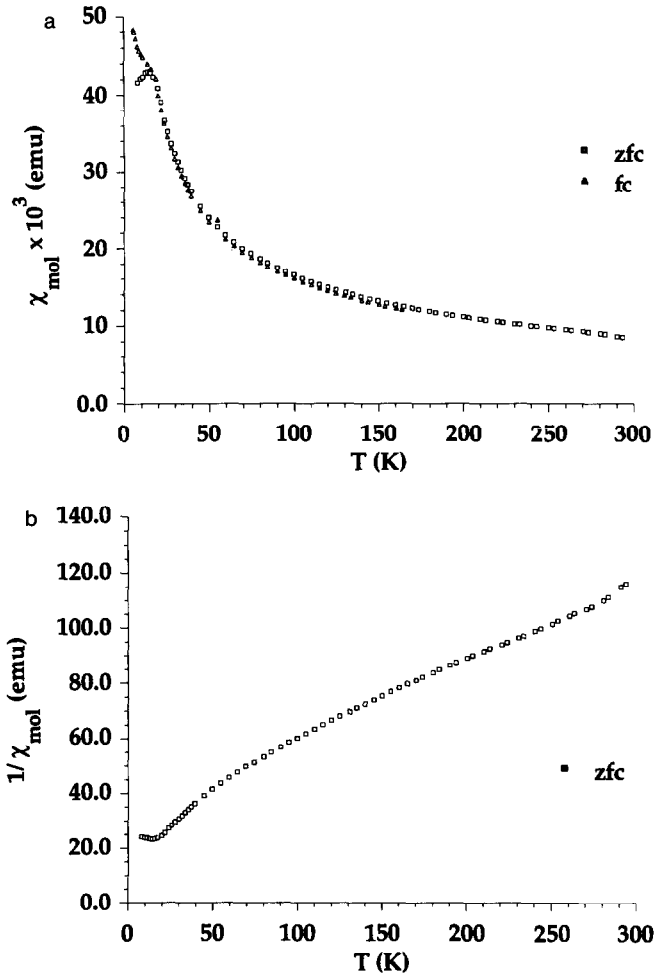

FIG. 5. (a) The zfc and fc molar magnetic susceptibility of Sr_4FeRuO_8 and (b) the zfc reciprocal susceptibility as a function of temperature.

the high-temperature magnetic susceptibility data suggest that short range antiferromagnetic order is present in both compounds at room temperature. This is not surprising in view of the strength of the nearest neighbour (nn) superexchange along Fe–O–Fe pathways that leads to a Néel temperature of 750 K in the perovskite $LaFeO_3$ (*8*). The changing gradient of the $1/\chi : T$ curve indicates that this short range coupling increases in strength at lower temperatures. In discussing our results on Sr_2FeRuO_6 we have previously argued (*1*) that the short-range antiferromagnetic coupling will be enhanced at low temperatures as the Fe–O–Fe interaction is reinforced by an antiferromagnetic Ru–O–Ru coupling. However, we also suggested that these interactions will be opposed by a ferromagnetic Fe–O–Ru interaction, and that the resulting frustration will lead to the observed spin glass behavior. The latter part of this argument is not entirely valid because, as we explained above, any six-coordinate site

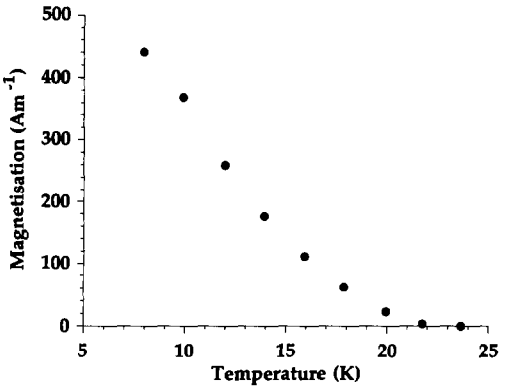

FIG. 6. The thermal remanent magnetization of Sr_3FeRuO_7 as a function of temperature.

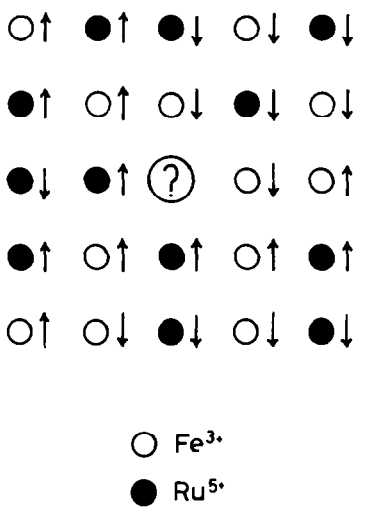

FIG. 7. Magnetic ordering of a random array of Fe^{3+} and Ru^{5+} cations on a square lattice with $J^{nn}_{Ru/Ru}$, $J^{nn}_{Fe/Fe} < 0$; $J^{nn}_{Fe/Ru} > 0$. The central cation will have spin up/down if it is Fe/Ru.

in these disordered structures can be occupied by either an Fe^{3+} cation or an Ru^{5+} cation in a magnetically ordered phase without frustration, and with the retention of the exchange constants $J^{nn}_{Ru/Ru}$, $J^{nn}_{Fe/Fe} < 0$; $J^{nn}_{Fe/Ru} > 0$, provided that the direction of the ordered magnetic moment at a site is reversed when the cation species occupying that site is changed. This is illustrated in Fig. 7. However, the discrepancy between the zfc and fc susceptibility data, the presence of a thermal remanent magnetization, and the absence of magnetic Bragg scattering at low temperatures all suggest that frustration is present in these compounds. In order to understand the source of the frustration we must consider the role of next-nearest-neighbor (nnn) cations. Figure 8 illustrates an extreme case in the two-dimensional structure of Sr_4FeRuO_8 where an Fe^{3+} cation has four nn Ru^{5+} ions and four nnn Fe^{3+} ions. If we only consider nn superexchange, then the magnetic structure shown in Fig. 8 results. However, this leaves the central Fe^{3+} cation ferromagnetically aligned with respect to four other Fe^{3+} ions in nnn sites. It has been established (*9*) that magnetic superexchange between cations of elements from the second transition series is very much weaker than that between cations of first row elements, and it is likely that the antiferromagnetic interaction between nnn Fe^{3+} cations is comparable in strength to both $J^{nn}_{Ru/Ru}$ and $J^{nn}_{Fe/Ru}$. The introduction of nnn interactions thus introduces frustration and explains the failure of these compounds to achieve long-range magnetic order. The more marked hysteresis in the magnetic susceptibility of Sr_4FeRuO_8 compared to that of Sr_3FeRuO_7 is consistent with this expla-

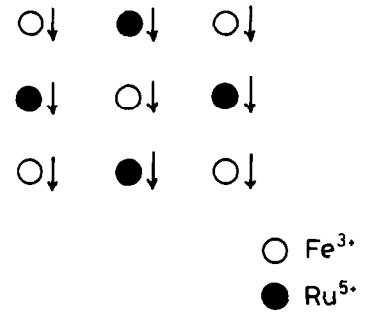

FIG. 8. The local magnetic structure around an Fe^{3+} cation with Ru^{5+} on all nn sites.

nation because, statistically, a larger fraction of the Fe^{3+} cations will have only Ru^{5+} cations as nearest neighbors in the two-dimensional structure as compared to the Ruddlesden–Popper structure, and the importance of the nnn interaction will thus be enhanced. Our model for these compounds thus involves the growth of essentially antiferromagnetic clusters with decreasing temperature, but with the establishment of long-range magnetic order frustrated by the presence of competing nn and nnn superexchange interactions. The competition arises because of the presence of two different cation species with different electron configurations (hence $J^{nn}_{Fe/Ru} > 0$) and with different magnitudes for their homoatomic exchange constants $J_{B/B}$; if $J_{Ru/Ru} \sim J_{Fe/Fe}$, then nearest-neighbor interactions would be expected to dominate completely those between next-nearest-neighbors. This is the case in the low-temperature phase of $BaLaFe_2O_{5.91}$ (*10, 11*), which contains a disordered 3 : 1 distribution of $Fe^{3+}:3d^5$ and $Fe^{5+}:3d^3$ (cf. $Ru^{5+}:4d^3$) over the six-coordinate sites of a simple cubic perovskite. This compound shows G-type long-range magnetic order, in which nn superexchange is dominant, at temperatures below 220 K. The average ordered magnetic moment per cation, measured in a neutron diffraction experiment, is considerably lower than the concentration-weighted mean of $\mu(Fe^{3+})$ and $\mu(Fe^{5+})$, and the data are therefore consistent with the presence of mixed ferromagnetic and antiferromagnetic coupling as drawn in Fig. 7. The involvement of two cations from the first transition series, rather than one from each of the first and second, ensures that all nn interactions are stronger than any nnn interactions, and thus there is no significant frustration, in contrast to the situation in mixed Fe/Ru oxides.

Acknowledgments

We are grateful to Dr. J. K. Cockcroft for experimental assistance at ILL Grenoble, and to the Science and Engineering Research Council for financial support.

References

1. P. D. BATTLE, T. C. GIBB, C. W. JONES, AND F. STUDER, *J. Solid State Chem.* **78,** 281 (1989).
2. J. B. GOODENOUGH, "Magnetism and the Chemical Bond," Wiley, New York (1963).
3. S. N. RUDDLESDEN AND P. POPPER, *Acta Crystallogr* **11,** 54 (1958).
4. R. GREATREX, N. N. GREENWOOD, AND M. LAL, *Mater. Res. Bull.* **15,** 113 (1980).
5. H. M. RIETVELD, *J. Appl. Crystallogr.* **2,** 65 (1969).
6. B. TOBY, D. E. COX, AND P. ZOLLIKER, unpublished work.
7. M. P. ATTFIELD, P. D. BATTLE, S. K. BOLLEN, S. H. KIM, A. V. POWELL, AND M. WORKMAN, *J. Solid State Chem.*, **96,** 344 (1992).
8. W. C. KOEHLER AND E. O. WOLLAN, *J. Phys. Chem. Solids* **2,** 100 (1957).
9. P. D. BATTLE, J. B. GOODENOUGH, AND R. PRICE, *J. Solid State Chem.* **46,** 234 (1983).
10. T. C. GIBB AND M. MATSUO, *J. Solid State Chem.* **81,** 83 (1989).
11. P. D. BATTLE, T. C. GIBB, P. LIGHTFOOT AND M. MATSUO, *J. Solid State Chem.* **85,** 38 (1990).